XXXVI Ibero-Latin American Congress on Computational Methods in Engineering
CILAMCE
Rio de Janeiro, 22-25 Nov 2015

PREDICTOR-MULTICORRECTOR SCHEMES FOR THE MULTISCALE DYNAMIC DIFFUSION METHOD TO SOLVE COMPRESSIBLE FLOW PROBLEMS

Ramoni Zancanela Sedano

rsedano@inf.ufes.br

Sérgio Souza Bento

sergio.bento@ufes.br

Leonardo Muniz de Lima

lmuniz@ifes.edu.br

Lucia Catabriga

luciac@inf.ufes.br

Universidade Federal do Espírito Santo

Av. Fernando Ferrari, 514, Goiabeiras, CEP 29075-910, Vitória - ES, Brazil

Abstract. *In this work we evaluate the predictor-multicorrector integration schemes for compressible Euler equations using the Dynamic Diffusion (DD) two-scale stabilized method. This multiscale finite element formulation is a free parameter method in which the subgrid scale space is defined using bubble functions whose degrees of freedom are locally eliminated in favor of the degrees of freedom that live on the resolved scales. The time advancing schemes assume that the resolved coarse scale chances in time by second order approximation and the unresolved scale can chance by first and second order approximations. The formulation is compared with the well known method SUPG considering two shock capturing operators, the Consistent Approximate Upwind Petrov-Galerkin (CAU) and the YZβ. Performance and accuracy comparisons are based on 2D test problems involving supersonic flows and shocks.*

Keywords: *Predictor-Multicorrector, Dynamic Diffusion Method, Compressible Euler Equations*

1 INTRODUCTION

The numerical solution of transport equations and inviscid compressible flows using the Galerkin formulation may exhibit global spurious oscillations. More accurate and stable results can be obtained using stabilized formulations, either linear or nonlinear approach (Brooks & Hughes, 1982; Hughes & Tezduyar, 1984; Hughes et al., 1989; Le Beau & Tezduyar, 1991; Franca & Valentin, 2000; Tezduyar & Senga, 2007; Catabriga et al., 2009; John & Knobloch, 2007; Hughes et al., 1986) and more recently stabilized formulation method have been reformulated considering variational multiscale formulations (Hughes, 1995; Franca et al., 1998; Hou & Wu, 1997; Guermond, 1999; Koobus & Farhat, 2004; Codina et al., 2007; Nassehi & Parvazinia, 2009; Gravemeier et al., 2010).

The multiscale approach consists of decomposing the approximation space into a resolved coarse scale and an unresolved subgrid scale spaces such that the weak form of the problem is split into two sub-problems: one for the coarse scales and one for the subgrid scales. From this point of view, the attempts to recover stability of the resolved scale solution may be interpreted as a way of improving the simulation by considering the effects of the smallest scales on the larger ones (Brezzi et al., 2003). In a general sense, each of these alternative methodologies are based on adding some type of stabilization to the standard Galerkin formulation and usually depends on the definition of one or more tuning parameters that usually play crucial role on the accuracy of the final solution.

The Nonlinear Subgrid Stabilization (NSGS) method, proposed by Santos & Almeida (2007), is a step towards the development of two-scale methods whose stability and convergence properties do not rely on tune-up parameters. It was based on adding a nonlinear artificial viscosity term only to the subgrid scales. The amount of the subgrid viscosity depends on assuming an additive decomposition of the velocity field and solving the resolved scale equation at the element level, yielding a self adaptive method. According to Santos et al. (2012), for advection-diffusion-reaction problems was proved that the NSGS is stable and yields optimal convergence rates by assuming that the grid is quasi-uniform, but presents the drawback of requiring the solution of a system twice as large as that associated with the resolved scale resolution.

Motivated by eddy viscosity models in which the dissipation mechanism is introduced either on all scales or on the subgrid scale, Arruda et al. (2010) proposed a discontinuous two scale method where an artificial diffusion appears on all scales, named Dynamic Diffusion method (DD). The additional diffusion is dynamically determined by imposing some restrictions on the resolved scale solution in the same spirit of the NSGS method. The DD method results in a free parameter method in which an artificial diffusion model acts isotropically and is locally adapted to guarantee stability of the resolved scale solution. The methodology outperforms some subgrid diffusion approaches for transport problems as well as some discontinuous capturing methods. In particular, it reformulates, using broken spaces, the Consistent Approximate Upwind Petrov-Galerkin (CAU) finite element model (Galeão & Carmo, 1988).

In this work we extend the DD to compressible Euler equations, applying the well known implicit predictor-multicorrector algorithm. The unresolved scale solution is advanced in time with two adaptations. Firstly, the unresolved scale is performed by first order approximation – denoted by DD-FP (Diffusion Dynamic First Order Predictor) – and also, we considerer second order approximation – denoted by DD-SP (Diffusion Dynamic Second Order Predictor). The formulation is compared with the well known method SUPG considering two shock capturing operators, the Consistent Approximate Upwind Petrov-Galerkin – denoted by SUPG/CAU – and the YZβ (Tezduyar & Senga, 2007) – denoted by SUPG/YZβ. Performance and accuracy comparisons are based on benchmark 2D problems.

2 Governing Equations

The two-dimensional Euler equations in conservation variables, $\boldsymbol{U} = (\rho, \rho u, \rho v, \rho e)$, without source terms are an inviscid system of conservation laws represented by

$$\boldsymbol{U}_{,t} + \boldsymbol{F}_{x,x} + \boldsymbol{F}_{y,y} = \mathbf{0} \text{ on } \Omega \times [0, T_f]. \tag{1}$$

where ρ is the fluid density, $\boldsymbol{u} = (u, v)$ is the velocity vector, e is the total energy per unit mass, $\boldsymbol{F}_x$ and $\boldsymbol{F}_y$ are the Euler fluxes, Ω is a domain in $\mathbb{R}^2$, and T_f is a positive real number. Alternatively, Eq. (1) can be written as

$$\boldsymbol{U}_{,t} + \boldsymbol{A}_x \boldsymbol{U}_{,x} + \boldsymbol{A}_y \boldsymbol{U}_{,y} = \mathbf{0} \text{ on } \Omega \times [0, T_f], \tag{2}$$

where $\boldsymbol{A}_x = \frac{\partial \boldsymbol{F}_x}{\partial \boldsymbol{U}}$ and $\boldsymbol{A}_y = \frac{\partial \boldsymbol{F}_y}{\partial \boldsymbol{U}}$. Associated to Eq. (2) we have proper set of boundary and initial conditions.

3 Finite Element Formulations

To define the finite element discretization, consider a triangular partition $\mathcal{T}_H$ of the domain Ω into n_{el} elements, where: $\Omega = \bigcup_{e=1}^{n_{el}} \Omega_e$ and $\Omega_i \cap \Omega_j = \emptyset$, $i, j = 1, 2, \cdots, n_{el}, \quad i \neq j$. We introduce the following two spaces:

$$\begin{aligned} \mathcal{V}_h &= \{\mathbf{U}_h \in [H_h^1(\Omega)]^4 \quad | \quad \mathbf{U}_h|_{\Omega_e} \in [P^1(\Omega_e)]^4, \mathbf{U}_h \cdot \mathbf{e}_k = g_k(t) \text{ in } \Gamma_{g_k}\}, \\ \mathcal{V}_B &= \{\mathbf{U}_B \in [H_0^1(\mathcal{T}_H)]^4 \quad | \quad \mathbf{U}_B|_{\Omega_e} \in [span(\psi_B)]^4, \quad \forall \Omega_e \in \mathcal{T}_H\}. \end{aligned}$$

where $\mathbb{P}_1(\Omega_e)$ represents the set of first order polynomials in Ω_e and ψ_B is a bubble function ($0 \leq \psi_B \leq 1$ and $\psi_B \in H_0^1(\mathcal{T}_H)$). Moreover, we introduce an additional discrete space $\mathcal{V}_E$, such that the following decomposition holds:

$$\mathcal{V}_E = \mathcal{V}_h \oplus \mathcal{V}_B \,, \tag{3}$$

where $\mathcal{V}_h$ is the resolved (coarse) scale space whereas $\mathcal{V}_B$ is the subgrid (fine) scale space (Figure 1).

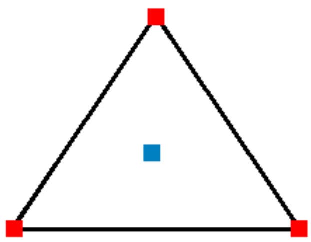

Figure 1. $\mathcal{V}_E$ **Representation**

The dynamic diffusion method for the Euler equation can be defined by find $\mathbf{U}_E = \mathbf{U}_h + \mathbf{U}_B \in \mathcal{V}_E$ with $\mathbf{U}_h \in \mathcal{V}_h$, $\mathbf{U}_B \in \mathcal{V}_B$ such that

$$\begin{aligned}
&\int_\Omega \mathbf{W}_E \cdot \Big(\frac{\partial \mathbf{U}_E}{\partial t} + \mathbf{A}_x^h \frac{\partial \mathbf{U}_E}{\partial x} + \mathbf{A}_y^h \frac{\partial \mathbf{U}_E}{\partial y}\Big) d\Omega \quad + \\
&\sum_{e=1}^{nel} \int_{\Omega_e} \zeta_h \Big(\frac{\partial \mathbf{W}_E}{\partial x} \cdot \frac{\partial \mathbf{U}_E}{\partial x} + \frac{\partial \mathbf{W}_E}{\partial y} \cdot \frac{\partial \mathbf{U}_E}{\partial y}\Big) d\Omega \quad = \quad \mathbf{0} \ \forall \mathbf{W}_E \in \mathcal{V}_E,
\end{aligned} \tag{4}$$

where $\mathbf{W}_E = \mathbf{W}_h + \mathbf{W}_B \in \mathcal{V}_E$ with $\mathbf{W}_h \in \mathcal{V}_h$, $\mathbf{W}_B \in \mathcal{V}_B$ and

$$\zeta_h = \zeta_h(\mathbf{U}_h) = \begin{cases} \frac{1}{2}\mu(h)\frac{\|R(\mathbf{U}_h)\|_{\widetilde{A}_0^{-1}}}{\|\boldsymbol{\nabla}_\xi \mathbf{U}_h\|_{\widetilde{A}_0^{-1}}}, \ \text{if } \|\boldsymbol{\nabla}\mathbf{U}_h\|_{\widetilde{A}_0^{-1}} > tol_\zeta; \\ \\ 0, \quad \text{otherwise}, \end{cases} \tag{5}$$

$\mu(h) = \sqrt{2A_e}$ is the element length, A_e is the element area, $\widetilde{\mathbf{A}}_0^{-1}$ is the Jacobian of the transformation between the entropy and conservation variables (Shakib et al., 1991),

$$R(\mathbf{U}_h) = \frac{\partial \mathbf{U}_h}{\partial t} + \mathbf{A}_x^h \frac{\partial \mathbf{U}_h}{\partial x} + \mathbf{A}_y^h \frac{\partial \mathbf{U}_h}{\partial y} \quad \text{on} \quad \Omega_e,$$

and

$$\|\boldsymbol{\nabla}_\xi \mathbf{U}_h\|_{\widetilde{A}_0^{-1}} = \left\| \frac{\partial x}{\partial \xi}\frac{\partial \mathbf{U}_h}{\partial x} + \frac{\partial y}{\partial \xi}\frac{\partial \mathbf{U}_h}{\partial y} \right\|_{\widetilde{A}_0^{-1}} + \left\| \frac{\partial x}{\partial \eta}\frac{\partial \mathbf{U}_h}{\partial x} + \frac{\partial y}{\partial \eta}\frac{\partial \mathbf{U}_h}{\partial y} \right\|_{\widetilde{A}_0^{-1}}.$$

When $\|\mathbf{U}_h\|_{\widetilde{A}_0^{-1}} \leq tol_\zeta$, the formulation (4) recovers the standard Galerkin method.

The DD method for the Euler equations is solved using iterative procedures for time and domain. The iterative procedure for domain is defined by given $\mathbf{U}_E^i$, we find $\mathbf{U}_E^{i+1}$ satisfying the formulation (4) where $\zeta_h = \zeta_h(\mathbf{U}_E^i) = \zeta_h^i$. The resulting formulation can be partitioned on resolved scale:

$$\begin{aligned}
&\int_\Omega \mathbf{W}_h \cdot \Big(\frac{\partial \mathbf{U}_h^{i+1}}{\partial t} + \mathbf{A}_x^h \frac{\partial \mathbf{U}_h^{i+1}}{\partial x} + \mathbf{A}_y^h \frac{\partial \mathbf{U}_h^{i+1}}{\partial y}\Big) d\Omega \quad + \\
&\int_\Omega \mathbf{W}_h \cdot \Big(\frac{\partial \mathbf{U}_B^{i+1}}{\partial t} + \mathbf{A}_x^h \frac{\partial \mathbf{U}_B^{i+1}}{\partial x} + \mathbf{A}_y^h \frac{\partial \mathbf{U}_B^{i+1}}{\partial y}\Big) d\Omega \quad + \\
&\sum_{e=1}^{nel} \int_{\Omega_e} \zeta_h^i \Big(\frac{\partial \mathbf{W}_h}{\partial x} \cdot \frac{\partial \mathbf{U}_h^{i+1}}{\partial x} + \frac{\partial \mathbf{W}_h}{\partial y} \cdot \frac{\partial \mathbf{U}_h^{i+1}}{\partial y}\Big) d\Omega \quad = \quad \mathbf{0}, \quad \forall \mathbf{W}_h \in \mathcal{V}_h,
\end{aligned} \tag{6}$$

and on subgrid scale:

$$\int_{\Omega} \mathbf{W}_B \cdot \frac{\partial \mathbf{U}_B^{i+1}}{\partial t} d\Omega + \int_{\Omega} \mathbf{W}_B \cdot \Big(\frac{\partial \mathbf{U}_h^{i+1}}{\partial t} + \mathbf{A}_x^h \frac{\partial \mathbf{U}_h^{i+1}}{\partial x} + \mathbf{A}_y^h \frac{\partial \mathbf{U}_h^{i+1}}{\partial y} \Big) d\Omega \quad +$$

$$\sum_{e=1}^{nel} \int_{\Omega_e} \zeta_h^i \Big(\frac{\partial \mathbf{W}_B}{\partial x} \cdot \frac{\partial \mathbf{U}_B^{i+1}}{\partial x} + \frac{\partial \mathbf{W}_B}{\partial y} \cdot \frac{\partial \mathbf{U}_B^{i+1}}{\partial y} \Big) d\Omega = \mathbf{0}, \quad \forall \mathbf{W}_B \in \mathcal{V}_B. \tag{7}$$

On Eqs. (6) and (7), the terms

$$\int_{\Omega_e} \zeta_h^i \Big(\frac{\partial \mathbf{W}_h}{\partial x} \cdot \frac{\partial \mathbf{U}_B^{i+1}}{\partial x} + \frac{\partial \mathbf{W}_h}{\partial y} \cdot \frac{\partial \mathbf{U}_B^{i+1}}{\partial y} \Big) d\Omega \text{ and } \int_{\Omega_e} \zeta_h^i \Big(\frac{\partial \mathbf{W}_B}{\partial x} \cdot \frac{\partial \mathbf{U}_h^{i+1}}{\partial x} + \frac{\partial \mathbf{W}_B}{\partial y} \cdot \frac{\partial \mathbf{U}_h^{i+1}}{\partial y} \Big) d\Omega$$

from the DD formulation and the convective term associated with the subgrid scale:

$$\int_{\Omega} \mathbf{W}_B \cdot \Big(\mathbf{A}_x^h \frac{\partial \mathbf{U}_B^{i+1}}{\partial x} + \mathbf{A}_y^h \frac{\partial \mathbf{U}_B^{i+1}}{\partial y} \Big) d\Omega$$

were omitted, once they are zero. Applying the standard finite element approximation on Eqs. (6) and (7), we arrive at a local system of ordinary differential equations:

$$\begin{bmatrix} M_{hh} & M_{hB} \\ M_{Bh} & M_{BB} \end{bmatrix} \begin{bmatrix} \dot{U}_h \\ \dot{U}_B \end{bmatrix} + \begin{bmatrix} K_{hh} & K_{hB} \\ K_{Bh} & K_{BB} \end{bmatrix} \begin{bmatrix} U_h \\ U_B \end{bmatrix} = \begin{bmatrix} 0_h \\ 0_B \end{bmatrix}, \tag{8}$$

where U_h and U_B are, respectively, the nodal values of the unknowns $\mathbf{U}_h$ and $\mathbf{U}_B$ on each element Ω_e, whereas $\dot{U}_h$ and $\dot{U}_B$ are its time derivative. The local matrices and vectors on the Eq. (8) are defined by:

$$M_{hh} \ : \ \int_{\Omega_e} \mathbf{W}_h \cdot \frac{\partial \mathbf{U}_h^{i+1}}{\partial t} d\Omega \tag{9}$$

$$M_{hB} \ : \ \int_{\Omega_e} \mathbf{W}_h \cdot \frac{\partial \mathbf{U}_B^{i+1}}{\partial t} d\Omega \tag{10}$$

$$M_{Bh} \ : \ \int_{\Omega_e} \mathbf{W}_B \cdot \frac{\partial \mathbf{U}_h^{i+1}}{\partial t} d\Omega \tag{11}$$

$$M_{BB} \ : \ \int_{\Omega_e} \mathbf{W}_B \cdot \frac{\partial \mathbf{U}_B^{i+1}}{\partial t} d\Omega \tag{12}$$

$$\begin{aligned} K_{hh} \ : \ & \int_{\Omega_e} \mathbf{W}_h \cdot \Big(\mathbf{A}_x^h \frac{\partial \mathbf{U}_h^{i+1}}{\partial x} + \mathbf{A}_y^h \frac{\partial \mathbf{U}_h^{i+1}}{\partial y} \Big) d\Omega + \\ & \int_{\Omega_e} \zeta_h^i \Big(\frac{\partial \mathbf{W}_h}{\partial x} \cdot \frac{\partial \mathbf{U}_h^{i+1}}{\partial x} + \frac{\partial \mathbf{W}_h}{\partial y} \cdot \frac{\partial \mathbf{U}_h^{i+1}}{\partial y} \Big) d\Omega \end{aligned} \tag{13}$$

$$K_{hB} \quad : \quad \int_{\Omega_e} \mathbf{W}_h \cdot \Big(\mathbf{A}_x^h \frac{\partial \mathbf{U}_B^{i+1}}{\partial x} + \mathbf{A}_y^h \frac{\partial \mathbf{U}_B^{i+1}}{\partial y} \Big) d\Omega \tag{14}$$

$$K_{Bh} \quad : \quad \int_{\Omega_e} \mathbf{W}_B \cdot \Big(\mathbf{A}_x^h \frac{\partial \mathbf{U}_h^{i+1}}{\partial x} + \mathbf{A}_y^h \frac{\partial \mathbf{U}_h^{i+1}}{\partial y} \Big) d\Omega \tag{15}$$

$$K_{BB} \quad : \quad \int_{\Omega_e} \zeta_h^i \Big(\frac{\partial \mathbf{W}_B}{\partial x} \cdot \frac{\partial \mathbf{U}_B^{i+1}}{\partial x} + \frac{\partial \mathbf{W}_B}{\partial y} \cdot \frac{\partial \mathbf{U}_B^{i+1}}{\partial y} \Big) d\Omega \tag{16}$$

Valli et al. (2014) and Valli et al. (2015) presented a predictor multi corrector algorithm considering first and second order approximations, respectively, for the unresolved scale applied to transport equations. In this study, we extended those ideas for the Euler equations. Algorithm 1 and 2 show, respectively, the first and second order approximations for the unresolved scale. In both algorithms: Δt is the time-step; subscripts $n+1$ and n mean, respectively, the solution on the time-step $n+1$ and n; α is the time advancing parameter, taken to be in interval $[0, 1]$; and the value $N_2 \neq 0$ for $\zeta_h > 0$.

Algorithm 1: DD-FP Algorithm

Step 1. $i = 0$ (i is the iteration counter)

Step 2. Predictor phase:

$U_h^{n+1,0} = U_h^n + (1-\alpha)\Delta t \dot{U}_h^n$,
$\dot{U}_h^{n+1,0} = 0$
$U_B^{n+1,0} = U_B^n$

Step 3. Multi corrector phase:

Residuo Force:
$R^{n+1,i} = F^{n+1} - (M\dot{U}_h^{n+1,i} + KU_h^{n+1,i})$,
with $M = M_{hh} - (M_{hB} + \Delta t K_{hB})(M_{BB} + \Delta t K_{BB})^{-1} M_{Bh}$,
$K = K_{hh} - (M_{hB} + \Delta t K_{hB})(M_{BB} + \Delta t K_{BB})^{-1} K_{Bh}$ and
$F^{n+1} = F_h + \frac{1}{\Delta t}[M_{hB} - (M_{hB} + \Delta t K_{hB})(M_{BB} + \Delta t K_{BB})^{-1} M_{BB}] U_B^{n+1,i}$

Solve:
$M^* \Delta \dot{U}_h^{n+1,i+1} = R^{n+1,i}$,
with $M^* = M + \alpha \Delta t K$

Corrector:
$U_B^{n+1,i+1} = (M_{BB} + \Delta t K_{BB})^{-1}[M_{BB} U_B^{n+1,i} - \Delta t(M_{Bh}\dot{U}_h^{n+1,i} + K_{Bh} U_h^{n+1,i})]$,
$U_h^{n+1,i+1} = U_h^{n,i} + \alpha \Delta t \Delta \dot{U}_h^{n+1,i+1}$,
$\dot{U}_h^{n+1,i+1} = \dot{U}_h^{n+1,i} + \Delta \dot{U}_h^{n+1,i+1}$

Algorithm 2: DD-SP Algorithm

Step 1. $i = 0 \quad$ (i is the iteration counter)

Step 2. Predictor phase:

$$U_h^{n+1,0} = U_h^n + (1-\alpha)\Delta t \dot{U}_h^n,$$
$$\dot{U}_h^{n+1,0} = 0$$
$$U_B^{n+1,0} = U_B^n + (1-\alpha)\Delta t \dot{U}_B^n,$$
$$\dot{U}_B^{n+1,0} = 0$$

Step 3. Multi corrector phase:

Residuo Force:

$$R_1^{n+1,i} = F_h^{n+1} - (M_{hh}\dot{U}_h^{n+1,i} + M_{hB}\dot{U}_B^{n+1,i}) - (K_{hh}U_h^{n+1,i} + K_{hB}U_B^{n+1,i})$$
$$R_2^{n+1,i} = F_B^{n+1} - (M_{Bh}\dot{U}_h^{n+1,i} + M_{BB}\dot{U}_B^{n+1,i}) - (K_{Bh}U_h^{n+1,i} + K_{BB}U_B^{n+1,i})$$

Solve:

$$M^*\Delta\dot{U}_h^{n+1,i+1} = F^*,$$

with $M^* = M_1 - N_1 N_2^{-1} M_2$ and $F^* = R_1 - N_1 N_2^{-1} R_2$

where $M_1 = M_{hh} + \alpha\Delta t K_{hh}$, $N_1 = M_{hB} + \alpha\Delta t K_{hB}$

$M_2 = M_{Bh} + \alpha\Delta t K_{Bh}$ and $N_2 = M_{BB} + \alpha\Delta t K_{BB}$

Corrector:

$$U_h^{n+1,i+1} = U_h^{n,i} + \alpha\Delta t\Delta\dot{U}_h^{n+1,i+1},$$
$$\dot{U}_h^{n+1,i+1} = \dot{U}_h^{n+1,i} + \Delta\dot{U}_h^{n+1,i+1}$$
$$U_B^{n+1,i+1} = U_B^{n,i} + \alpha\Delta t\Delta\dot{U}_B^{n+1,i+1},$$
$$\dot{U}_B^{n+1,i+1} = \dot{U}_B^{n+1,i} + \Delta\dot{U}_B^{n+1,i+1}$$

with $\Delta\dot{U}_B^{n+1,i+1} = N_2^{-1}(R_2^{n+1,i} - M_2\Delta\dot{U}_h^{n+1,i+1})$

4 Numerical Experiments

In this section we present numerical experiments considering two benchmarks problems: 2D oblique shock and 2D reflected shock. We compare the first and second predictor - multicorrector integration schemes for the Dynamic Diffusion formulation, respectively named DD-FP and DD-SP with the predictor-multicorrector scheme for the SUPG formulation with two shock capturing operators, respectively, CAU and YZβ, named, SUPG/CAU and SUPG/YZβ. The tolerance tol_ζ (Eq. (5)) is 10^{-10}, the GMRES tolerance is 10^{-1}, the dimension of the Krylov subspace is 5, the number of multicorrections fixed to 3, the time-step size is $\Delta t = 10^{-2}$ and the simulation is run until 300 steps. The tests were performed on a machine with a processor Intel Core i5-3570 3.4 GHz with 4GB of RAM and Ubuntu 14.04 operating system.

4.1 2D Reflected Shock

This problem consists of three regions (R1, R2 and R3) separated by an oblique shock and its reflection from a wall, as shown in Fig. 2. Prescribing the following Mach 2.9 inflow data in the first region on the left (R1), and requiring the incident shock to be at an angle of $29°$, leads to the following exact solution at the other two regions (R2 and R3):

$$\text{R1}\begin{cases} M &= 2.9 \\ \rho &= 1.0 \\ u &= 2.9 \\ v &= 0.0 \\ p &= 0.714286 \end{cases} \quad \text{R2}\begin{cases} M &= 2.3781 \\ \rho &= 1.7 \\ u &= 2.61934 \\ v &= -0.50632 \\ p &= 1.52819 \end{cases} \quad \text{R3}\begin{cases} M &= 1.94235 \\ \rho &= 2.68728 \\ u &= 2.40140 \\ v &= 0.0 \\ p &= 2.93407 \end{cases} \tag{17}$$

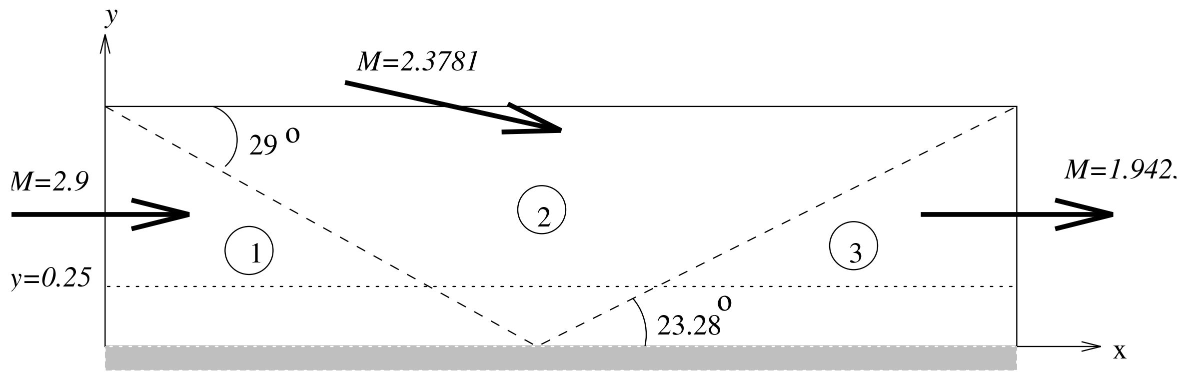

Figure 2. Reflected shock – problem description

The computational domain is a rectangle with $0 \leq x \leq 4.1$ and $0 \leq y \leq 1$. We prescribe the density, velocities and pressure at the left and top boundaries, the slip condition with $v = 0$ is imposed at the bottom boundary, and no boundary condition is imposed at the outflow (right) boundary. We use an unstructured mesh, refined in shock direction, with 2269 nodes and 4376 elements (see Fig. 3).

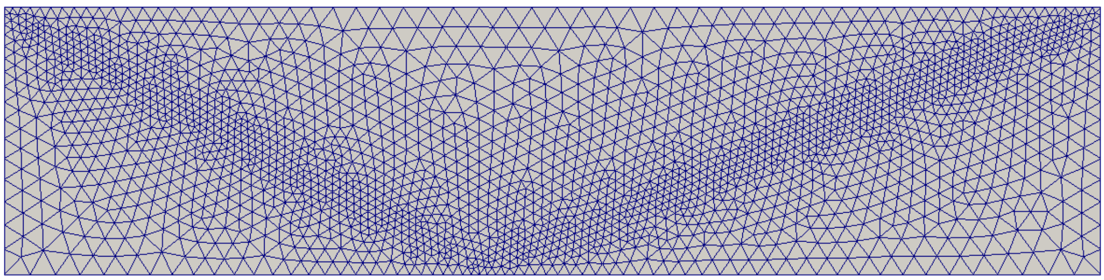

Figure 3. Unstructured mesh with 2269 nodes and 4376 elements – Reflected shock

Figure 4 shows the density distribution for the DD-FP (Fig. 4(a)) and DD-SP (Fig. 4(b)) scheme and Fig. 5 shows the density along line $y = 0.25$ considering the time advancing parameter $\alpha = 0.7$. The density profile for the DD-FP scheme shows some oscillations, although is closer to the exact profile when compared with the DD-SP scheme. It is important to note that the convergence is not achieved by the DD-FP scheme with $\alpha = 0.5$.

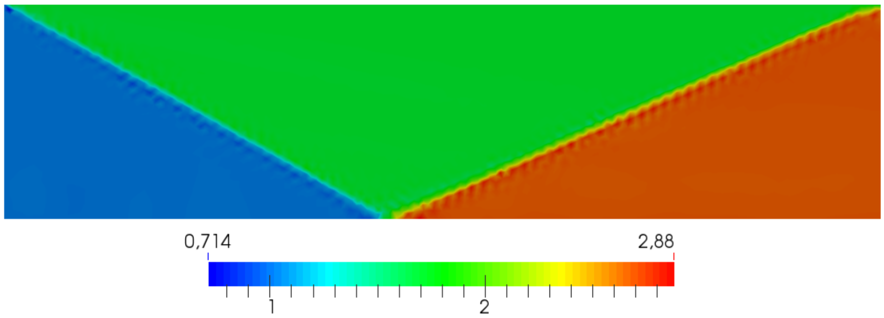

(a) DD-FP scheme

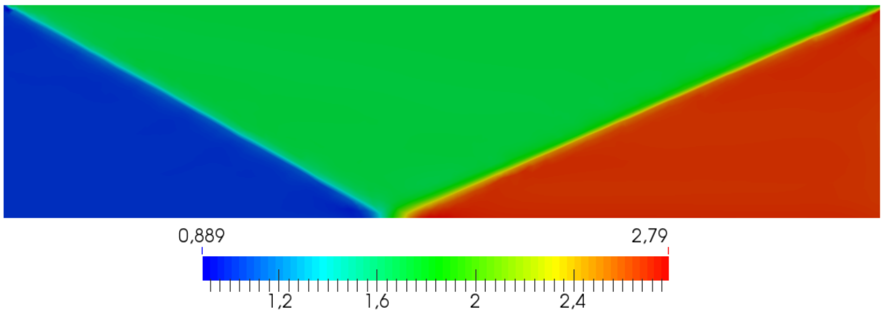

(b) DD-SP scheme

Figure 4. Density distribution with $\alpha = 0.7$ – Reflected shock

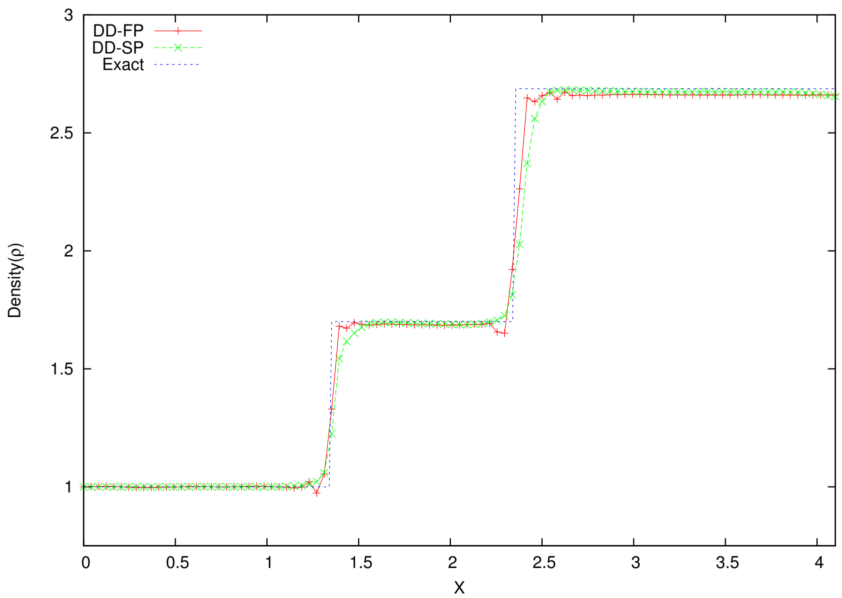

Figure 5. Density profile at $y = 0.25$ with $\alpha = 0.7$ – Reflected shock

Figure 6 shows the density along line $y = 0.25$ for the DD-SP, SUPG/CAU and SUPG/YZβ methods considering for all schemes $\alpha = 0.5$ – mesh and others parameters are the same of the previous experiment. As one can see, the solution are in good agreement with the exact solution, although all solutions have certain diffusivity at the shock regions. The SUPG/YZβ gives the better solution at the end of each region, while the DD-SP gives the better solution at the beginning of each region.

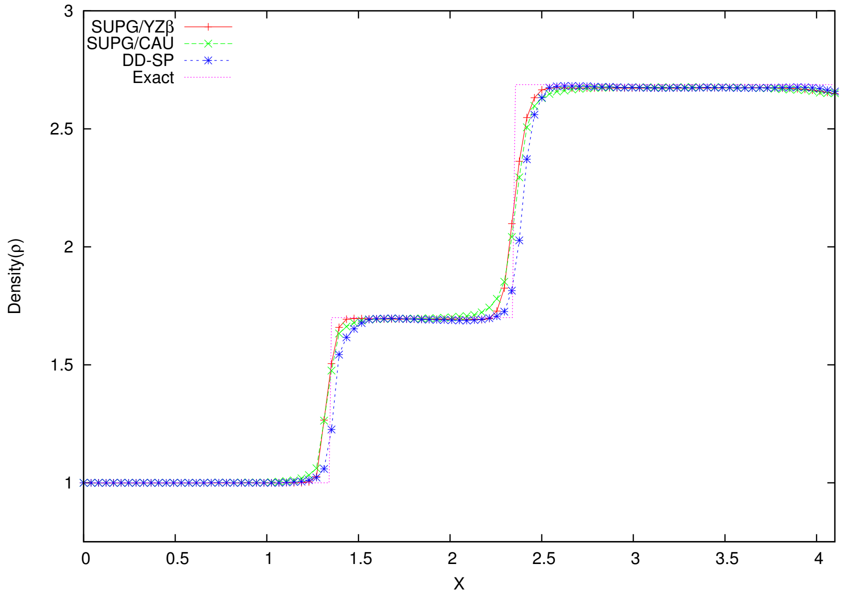

Figure 6. Density profiles at $y = 0.25$ with $\alpha = 0.5$ – Reflected shock

The number of GMRES iterations and the CPU time of the DD-SP, SUPG/CAU and SUPG/YZβ methods are shown in Table 1. The DD-SP scheme needs the smaller number of GMRES iterations – 13.26% less than the SUPG/YZβ and 63.22% less than the SUPG/CAU. Therefore the CPU time for the DD-SP scheme is faster than the SUPG/YZβ scheme (about 15%) and faster than the SUPG/CAU scheme (more than 50%).

Table 1. Computational Performance: mesh with 2269 nodes, 4376 elements and $\alpha = 0.5$ – Reflected shock

Methods	GMRES Iterations	CPU Time (s)
DD-SP	4808	32.245
SUPG/CAU	13073	67.692
SUPG/YZβ	5543	37.874

Figure 7 shows the evolution of the density residual for 300 steps for the DD-SP, SUPG/YZβ and SUPG/CAU schemes. The DD-SP residual evolution is much smaller than the others. This effect can justify the fact that the DD-SP scheme converges with fewer iterations.

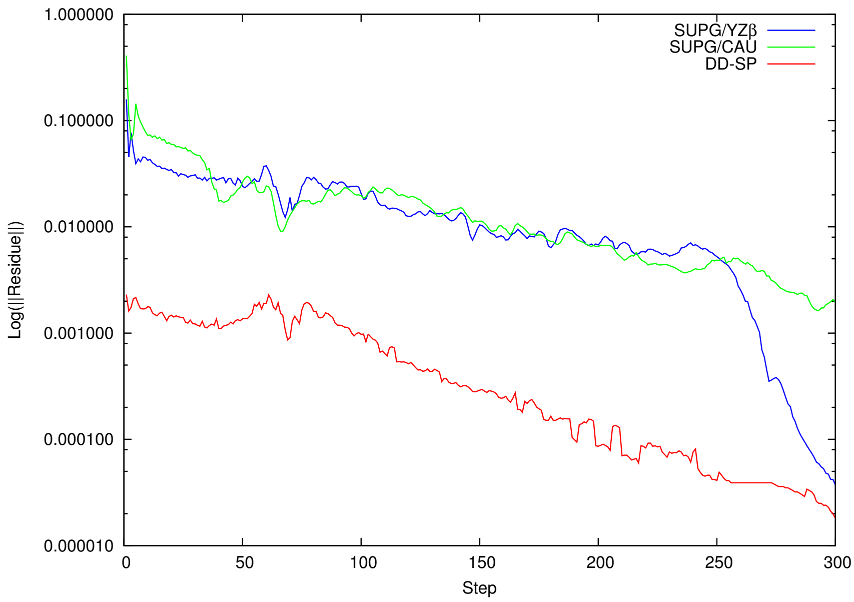

Figure 7. Evolution of density residual with $\alpha = 0.5$ – Reflected shock

4.2 2D Oblique Shock

The second problem is a Mach 2 uniform flow over a wedge, at an angle of $-10°$ with respect to a horizontal wall. The solution involves an oblique shock at an angle of $29.3°$ emanating from the leading edge of the wedge, as shown in Fig. 8.

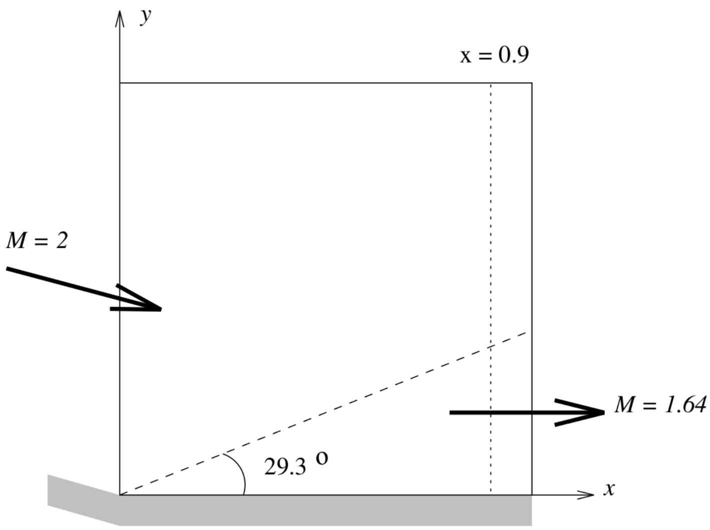

Figure 8. Oblique shock – problem description

The computational domain is a square with $0 \leq x \leq 1$ and $0 \leq y \leq 1$. Prescribing the following inflow data on the left and top boundaries results in a solution with the following outflow data:

$$\text{Inflow}\quad \begin{cases} M &= 2.0 \\ \rho &= 1.0 \\ u &= cos10^0 \\ v &= -sin10^0 \\ p &= 0.17857 \end{cases} \qquad \text{Outflow}\quad \begin{cases} M &= 1.64052 \\ \rho &= 1.45843 \\ u &= 0.88731 \\ v &= 0.0 \\ p &= 0.30475 \end{cases} \tag{18}$$

Here M is the Mach number and p is the pressure. Four Dirichlet boundary conditions are imposed at the left and top boundaries, the slip condition with $v = 0$ is set at the bottom boundary, and no boundary condition is imposed at the outflow (right) boundary. We use an unstructured mesh, refined in shock direction, with 2545 nodes and 4966 elements (see Fig. 9).

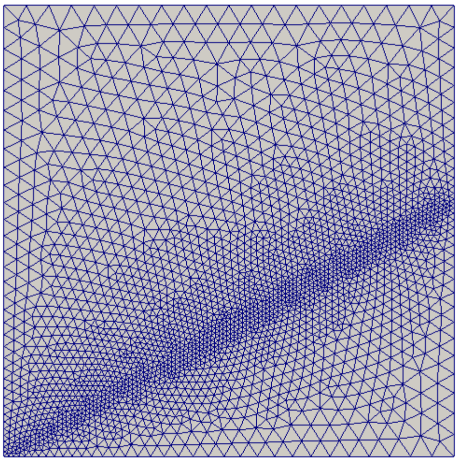

Figure 9. Unstructured mesh with 2545 nodes and 4966 elements – Oblique shock

Figure 10 show the density distribution for the DD-SP, SUPG/CAU and SUPG/YZβ scheme considering $\alpha = 0.5$. Unfortunately, the DD-SP scheme does not reach an accuracy like the others and the DD-FP scheme does not converge. In Fig. 10(a) we can see some oscillations through shock region, whereas Fig. 10(b) and Fig. 10(c) present a high quality solution.

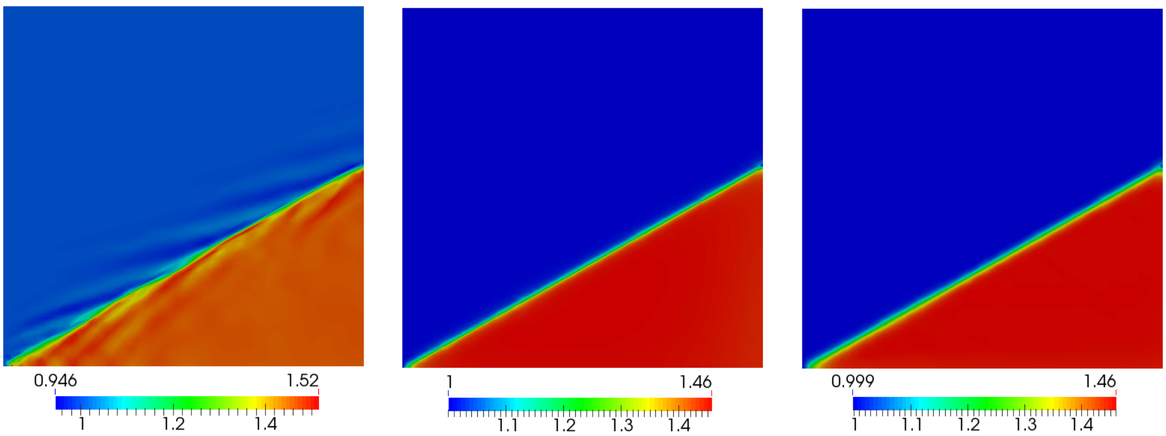

(a) DD-SP scheme (b) SUPG/CAU scheme (c) SUPG/YZβ scheme

Figure 10. Density distribution with $\alpha = 0.5$ – Oblique shock

By analyzing the density profile at $x = 0.9$, as shown in Fig. 11, we conclude that the DD-SP scheme does not suppress oscillations as in the reflected shock problem. In this case, the formulations based on SUPG formulations obtained better results.

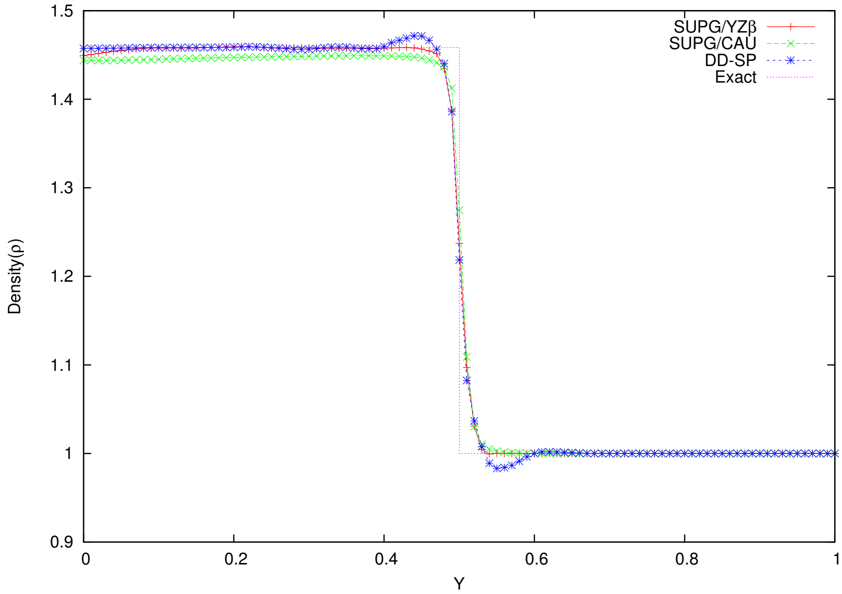

Figure 11. Density profile at $x = 0.9$ with $\alpha = 0.5$ – Oblique shock

The number of GMRES iterations and the CPU time of the DD-SP, SUPG/CAU and SUPG/YZβ methods are shown in Table 2. The SUPG/YZβ scheme needs the smallest number of GMRES iterations and the SUPG/CAU the largest. The number of GMRES iteration of the DD-SP scheme is almost 54% larger than the number of GMRES iterations of the SUPG/YZβ scheme, while the CPU time is less than 11%. Thus, the DD-SP CPU time for each iteration is less expensive than the SUPG/YZβ CPU time.

Table 2. Computational Performance: mesh with 2545 nodes, 4966 elements and $\alpha = 0.5$ – Oblique shock

Methods	GMRES Iterations	CPU Time (s)
DD-SP	12019	58.533
SUPG/CAU	26232	129.480
SUPG/YZβ	7816	52.797

Figure 12 shows the evolution of the density residual for 300 steps for the DD-SP, SUPG/YZβ and SUPG/CAU schemes. Once again, the residual norm of the DD-SP method is smaller than the SUPG based methods.

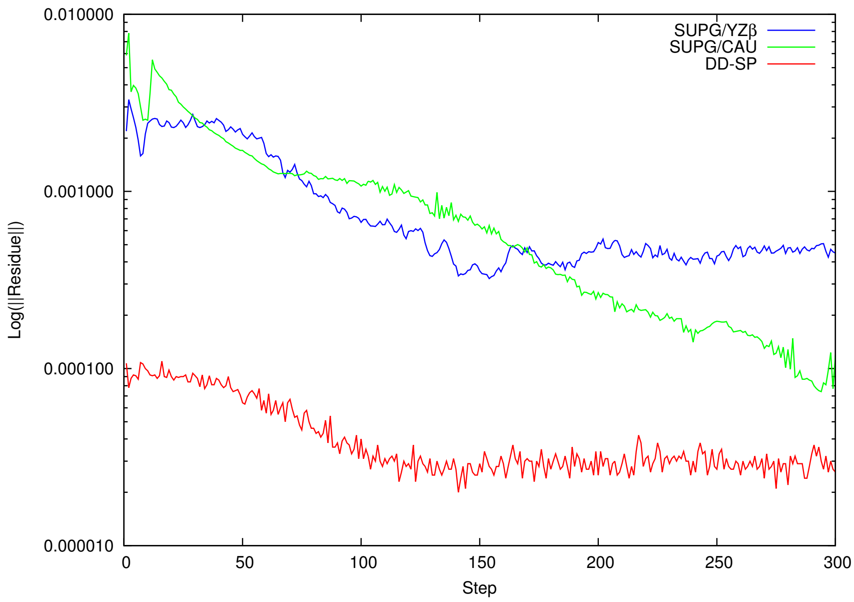

Figure 12. Evolution of density residual with $\alpha = 0.5$ – Oblique shock

5 Conclusions

In this work, we evaluated two schemes for the compressible Euler equations. One is the DD-FP scheme using a first order approximation in the unresolved scale of the DD formulation. The other is the DD-SP scheme using a second order approximation in the unresolved scale. We compared those schemes by running the well known benchmark problem reflected shock. The DD-SP scheme reached advantages once it did not present spurious modes. In addition, the DD-SP scheme was compared with the SUPG formulation considering two shock capturing operators, CAU and YZβ. The DD-SP presented no oscillations as well as the SUPG/CAU and SUPG/YZβ schemes with fewer GMRES iterations and less CPU time. We also simulated another well known benchmark problem oblique shock, where the DD-FP scheme did not work and the DD-SP did not live up to expectations compared to the SUPG/CAU and SUPG/YZβ formulations. Although the DD-SP scheme has made some improvements over the DD-FP scheme, it was not sufficient to classify it as a robust method as well as the SUPG/CAU and the SUPG/YZβ methods for compressible Euler equations. However, we plan to investigate the DD schemes considering local time-stepping strategies and procedures to freeze the amount of artificial diffusivity to be added by numerical model.

ACKNOWLEDGEMENTS

This work has been supported in part by CNPq, CAPES and FAPES.

REFERENCES

Arruda, N. B., Almeida, R. C. & do Carmo, E. G. D., 2010. Dynamic diffusion formulations for advection dominated transport problems, *Mecânica Computacional* 29, 2011–2025.

Brezzi, F., Marini, L. D. & Sangalli, G., 2003. Link-cutting bubbles for the stabilization of convection-diffusion-reaction problems, *Mathematical Models and Methods in Applied Science* 13, 445–461.

Brooks, A. N. & Hughes, T. J. R., 1982. Streamline upwind Petrov-Galerkin formulations for convection dominated flows with particular emphasis on the incompressible Navier-Stokes equations, *Computer Methods in Applied Mechanics and Engineering* 32, 199–259.

Catabriga, L., de Souza, D. A., Coutinho, A. L. & Tezduyar, T. E., 2009. Three-dimensional edge-based supg computation of inviscid compressible flows with yzβ shock-capturing, *Journal of Applied Mechanics* 76(2), 021208.

Codina, R., Principe, J., Guasch, O. & Badia, S., 2007. Time dependent subscales in the stabilized finite element approximation of incompressible flow problems, *Computer Methods in Applied Mechanics and Engineering* 196, 2413–2430.

Franca, L. P., Nesliturk, A. & Stynes, M., 1998. On the stability of residual-free bubbles for convection-diffusion problems and their approximation by a two-level finite element method, *Computer Methods in Applied Mechanics and Engineering* 166, 35–49.

Franca, L. P. & Valentin, F., 2000. On an improved unusual stabilized finite element method for the advective–reactive–diffusive equation, *Computer Methods in Applied Mechanics and Engineering* 190(13), 1785–1800.

Galeão, A. & Carmo, E., 1988. A consistent approximate upwind petrov-galerkin method for convection-dominated problems, *Computer Methods in Applied Mechanics and Engineering* 68, 83–95.

Gravemeier, V., Gee, M. W., Kronbichler, M. & Wall, W. A., 2010. An algebraic variational multiscale–multigrid method for large eddy simulation of turbulent flow, *Computer Methods in Applied Mechanics and Engineering* 199(13), 853–864.

Guermond, J.-L., 1999. Stabilization of galerkin approximations of transport equations by subgrid modeling, *ESAIM: Mathematical Modelling and Numerical Analysis* 33(06), 1293–1316.

Hou, T. Y. & Wu, X.-H., 1997. A multiscale finite element method for elliptic problems in composite materials and porous media, *Journal of computational physics* 134(1), 169–189.

Hughes, T. J., Franca, L. & Mallet, M., 1986. A new finite element formulation for computational fluid dynamics: I. symmetric forms of the compressible euler and navier-stokes equations and the second law of thermodynamics, *Computer Methods in Applied Mechanics and Engineering* 54(2), 223–234.

Hughes, T. J. R., 1995. Multiscale phenomena: Green's functions, the dirichlet-to-neumann formulation, sugrid scale models, bubbles and the origin of stabilized methods, *Computer Methods in Applied Mechanics and Engineering* 127, 387–401.

Hughes, T. J. R., Franca, L. P. & Hulbert, G. M., 1989. A new finite element formulation for computational fluid dynamics: Viii. the galerkin-least-squares method for advective-diffusive equations, *Computer Methods in Applied Mechanics and Engineering* 73, 173–189.

Hughes, T. J. & Tezduyar, T., 1984. Finite element methods for first-order hyperbolic systems with particular emphasis on the compressible euler equations, *Computer methods in applied mechanics and engineering* 45(1), 217–284.

John, V. & Knobloch, P., 2007. On spurious oscillations at layers diminishing (sold) methods for convection–diffusion equations: Part i–a review, *Computer Methods in Applied Mechanics and Engineering* 196(17), 2197–2215.

Koobus, B. & Farhat, C., 2004. A variational multiscale method for the large eddy simulation of compressible turbulent flows on unstructured meshes—-application to vortex shedding, *Computer Methods in Applied Mechanics and Engineering* 193(15), 1367–1383.

Le Beau, G. & Tezduyar, T., 1991. Finite element solution of flow problems with mixed-time integration, *Journal of engineering mechanics* 117(6), 1311–1330.

Nassehi, V. & Parvazinia, M., 2009. A multiscale finite element space–time discretization method for transient transport phenomena using bubble functions, *Finite Elements in Analysis and Design* 45(5), 315–323.

Santos, I., Almeida, R. & Malta, S., 2012. Numerical analysis of the nonlinear subgrid scale method, *Computational & Applied Mathematics* 31(3), 473–503.

Santos, I. P. & Almeida, R. C., 2007. A nonlinear subgrid method for advection-diffusion problems, *Computer Methods in Applied Mechanics and Engineering* 196, 4771–4778.

Shakib, F., Hughes, T. J. & Johan, Z., 1991. A new finite element formulation for computational fluid dynamics: X. the compressible euler and navier-stokes equations, *Computer Methods in Applied Mechanics and Engineering* 89(1), 141–219.

Tezduyar, T. E. & Senga, M., 2007. Supg finite element computation of inviscid supersonic flows with yzβ shock-capturing, *Computers & fluids* 36(1), 147–159.

Valli, A. M. P., Catabriga, L., Santos, I. P., Coutinho, A. L. G. A. & Almeida, R. C., 2014. Time integration schemes for a multiscale finite element formulation to solve transient advection-diffusion-reaction problems, *CILAMCE 2014* .

Valli, A. M. P., Catabriga, L., Santos, I. P., Coutinho, A. L. G. A. & Almeida, R. C., 2015. Predictor-multicorrector scheme for the dynamic diffusion method. accepted for *Proceeding Series of the Brazilian Society of Computational and Applied Mathematics*.